



## Abstract

We conducted the first ever mercury speciation measurements atop the Greenland ice sheet at Summit Station (Latitude 72.6° N, Altitude 3200 m) in the Spring and Summer of 2007 and 2008. These measurements were part of the GSHOX campaigns investigating the importance of halogen chemistry in this remote environment. Significant levels of BrO (1–5 pptv) in the near surface air were often accompanied by depletions of gaseous elemental mercury (GEM) below background levels, and in-situ production of reactive gaseous mercury (RGM). While halogen (i.e. Br) chemistry is normally associated with marine boundary layers, at Summit, Greenland, far from any marine source, we have conclusively detected bromine and mercury chemistry in the near surface air. We suggest that the fate of the formed mercury-bromine radical (HgBr) is further oxidation to stable RGM (HgBr<sub>2</sub>, HgBrOH, HgBrCl, etc.), or thermal decomposition. These fates appear to be controlled by the availability of Br, OH, Cl, etc. to produce RGM (Hg(II)), versus the lifetime of HgBr by thermal dissociation. At Summit, the availability of Br appears to be controlled by J(Br<sub>2</sub>), requiring a sun angle of > 5 degrees, while the formation of RGM from HgBr requires a temperature < -15°C. The majority of the deposited RGM is readily photoreduced and re-emitted to the air as GEM. However, a very small fraction becomes buried at depth. Extrapolating to the entire Greenland ice sheet, we calculate an estimated net annual sequestration of ~ 13 metric tons Hg per year, buried long-term under the sunlit photoreduction zone.

## 1 Introduction

In Spring 2007 and again in Spring/Summer 2008 we conducted the first ever mercury speciation measurements atop the Greenland ice sheet at Summit Station (Latitude 72.6° N, Altitude 3200 m). These measurements were part of the larger GSHOX campaigns investigating the importance of halogens in this remote environment. Significant levels of BrO (1–5 pptv) were observed in the near surface air utilizing both a differential

ACPD

11, 3663–3691, 2011

## Temperature and sunlight controls of mercury oxidation and deposition

S. Brooks et al.

Title Page

Abstract

Introduction

Conclusions

References

Tables

Figures

⏪

⏩

◀

▶

Back

Close

Full Screen / Esc

Printer-friendly Version

Interactive Discussion



optical absorption spectrometer (DOAS) and a chemical ionization mass spectrometer (CIMS). The presence of Br chemistry in the near surface air was most often accompanied by a decrease in concentration of gaseous elemental mercury (GEM) below background levels, and simultaneous in-situ production of reactive gaseous mercury (RGM). This chemical phenomenon is termed an atmospheric mercury depletion event (AMDE). These events have been found to be common at polar coastal and marine locations. Here we report the first Hg speciation measurements to demonstrate that AMDE chemistry occurs at the top of the Greenland ice sheet, nearly 1000 km from the nearest marine environment.

Summit is a remote camp several hundreds of kilometers from any population or infrastructure. Mercury emissions from the camp itself were not detected. All atmospheric sampling was conducted in the clean air sector at an all-electric satellite camp located roughly 1.5 km South-Southwest of the main Summit Station. Wind direction at Summit is seldom from the North, placing our atmospheric sampling predominately on the upwind side of main station.

Previous atmospheric chemistry investigations at Summit (Sjostedt et al., 2007) had hinted at active bromine chemistry, but showed no direct evidence and questionable mechanisms for Br transport to Summit. Here we confirm active Br + Hg chemistry at Summit, although the specific pathway(s) for Br transport to the site are yet to be fully understood.

## 2 Prior polar mercury measurements

The initial discovery of AMDEs was made in Alert, Canada in 1995 (Schroeder et al., 1998). It was shown that GEM was oxidized and deposited onto arctic snow surfaces more rapidly than was previously thought possible. In recent years, AMDEs have been observed at a variety of polar coastal sites including Barrow, Alaska (Lindberg et al., 2002), Neumeyer, Antarctica (Ebinghaus et al., 2002), Ny-Ålesund, Svalbard (Berg et al., 2003), Station Nord, Greenland (Skov et al., 2004), and Amderma, Russia (Steffen

### Temperature and sunlight controls of mercury oxidation and deposition

S. Brooks et al.

Title Page

Abstract

Introduction

Conclusions

References

Tables

Figures

⏪

⏩

◀

▶

Back

Close

Full Screen / Esc

Printer-friendly Version

Interactive Discussion



et al., 2005). More recently Brooks et al. (2008) and Dommergue et al. (2010) reported AMDE-like mercury oxidation and deposition atop the Antarctic ice sheet at South Pole and the French-Italian Concordia Base, respectively.

In general, it has been determined that polar AMDEs result from GEM/halogen chemistry (Steffen et al., 2008), and are confined to the shallow atmospheric boundary layer (typically less than a few hundreds of meters; Banic et al., 2003; Tackett et al., 2007). AMDEs are considered the predominate pathway for mercury deposition to the polar regions as GEM itself does not condense or dry deposit, and is not significantly adsorbed onto snow and ice surfaces (Bartels-Rauch et al., 2002; Ferrari et al., 2004). Deposition from AMDEs can dramatically increase mercury concentrations in the surface snow up to  $500 \text{ ng l}^{-1}$  (Lindberg et al., 2002; Lu et al., 2002; Brooks et al., 2006). However, it has also been observed that, within hours of deposition under sunlit conditions, the majority of the deposited Hg is photoreduced and re-emitted as GEM back to the atmosphere (Lalonde et al., 2002; Lalonde et al., 2003; Dommergue et al., 2003). Net deposition relies on mercury-rich snow becoming buried below the sunlit layer ( $\sim 10 \text{ cm}$ ; King and Simpson, 2001) by drifts or additional snowfall (Brooks et al., 2008). Estimates of net deposition to the Arctic are therefore difficult. A current estimate of 300 metric tons Hg per year was suggested by Ariya et al. (2004). The observations reported here, indicating that AMDE chemistry and deposition occur atop the Greenland ice sheet, will upwardly revise this estimate for the Arctic by  $\sim 4\text{--}5\%$ .

### 3 Implications

Increasingly, ice cores from Greenland and Antarctica are being used to elucidate the atmospheric and climate history of this planet. While mercury data from the ice sheet corings are sparse, pre-industrial mercury net deposition from ice coring, covering the past 34 000 years, show that mercury deposition was highest during the last glacial maximum (Vandal et al., 1993). Post-industrial ice coring in Greenland, showing mercury deposition from 1949 to 1989, indicate higher net deposition rates in the 50's and

## Temperature and sunlight controls of mercury oxidation and deposition

S. Brooks et al.

Title Page

Abstract

Introduction

Conclusions

References

Tables

Figures



Back

Close

Full Screen / Esc

Printer-friendly Version

Interactive Discussion



60's followed by a decrease in recent years (Boutron et al., 1998; Mann et al., 2005). These higher levels in the 50's and 60's, followed by steadily decreasing levels, roughly correlate with the anthropogenic emissions trend in the Northern Hemisphere.

Mercury, as a stable element, is neither created nor destroyed. While other compounds within ice cores may change over time, total mercury concentrations will remain forever unaltered.

By understanding current Hg chemistry, deposition and burial, it may be possible that Hg recovered from Greenland ice cores along with other species, may indicate past gaseous elemental mercury concentrations, snow burial rates, and/or halogen chemistry levels.

## 4 Measurements

Our mercury speciation sensor suite consisted of Tekran models 2537a/1130/1135 for the determination of gaseous elemental mercury (GEM, Hg<sup>0</sup>), reactive gaseous mercury (RGM, Hg(II,g)), and fine particulate mercury (FPM, Hg(II,p)), respectively (Fitzgerald and Gill, 1979; Lu et al., 1998; Landis et al., 2002).

The system was set to collect RGM and FPM for one hour, while concurrently collecting and analyzing 5-min GEM samples. At the end of the sampling hour, the system analyzed the preconcentrated RGM and FPM over the following hour. The resultant dataset consists of 12 one-hour RGM and FPM samples daily, and the same 12 h of 5-min GEM samples. Effectively, the sampling system runs 50% of the time and analyzes, without sampling, 50% of the time. Therefore, not all short duration (minutes to one hour) mercury events are captured.

Inlet air to the Tekran 1130 pump unit was pre-conditioned with a Tekran model 1102 air drier. The system was placed ~ 3 m South-Southwest of a small shelter at the satellite camp, with the inlet ~ 1.3 m above the surface. At this height the inlet was sufficiently above the blowing snow layer, but in the lowest few percent of the atmospheric boundary layer, which was often as shallow as a few tens of meters.

## Temperature and sunlight controls of mercury oxidation and deposition

S. Brooks et al.

Title Page

Abstract

Introduction

Conclusions

References

Tables

Figures

⏪

⏩

◀

▶

Back

Close

Full Screen / Esc

Printer-friendly Version

Interactive Discussion



## Temperature and sunlight controls of mercury oxidation and deposition

S. Brooks et al.

Title Page

Abstract

Introduction

Conclusions

References

Tables

Figures

⏪

⏩

◀

▶

Back

Close

Full Screen / Esc

Printer-friendly Version

Interactive Discussion



Specific care was taken for the cold, high-altitude environment. The case heaters for the 1130 and 1135 front end units were increased from 100 (standard) to 200 watts. Additional foam insulation was used to cover the bottom vented plate in the 1135 front end unit, and the side vent of the 1130 front end unit. These were done to minimize the variation in interior temperatures regardless of wind and weather conditions. Likewise, the heated sample lines were kept fully external to the climate controlled shelter. Otherwise, temperature changes between interior and exterior portions would induce hot/cold zones and mercury absorption/desorption at the tubing walls. To compensate for the high altitude of Summit, we reduced the mass flow through the system to maintain the  $\sim 0.1$  s designed residency time for ambient air over the KCl-coated annular denuder.

All snow samples were collected from the top 3–5 cm in pre-cleaned bottles using clean techniques and later analyzed for total mercury using EPA method 1631 (detection limit  $\sim 1$  ng l<sup>-1</sup>).

## 5 Quality assurance

The mercury system was leak tested and zero-air tested at least daily. The Tekran model 2537a internal permeation source calibrations were performed at 26-h intervals. All snow samples were refrigerated and hand-carried back to the analysis laboratory. Water blanks, bubbler blanks, and NIST standards were analyzed in conjunction with the samplers following EPA method 1631 for determining total mercury in the range of 0.5–100 ng l<sup>-1</sup> (Titled – Mercury in water by oxidation, purge, and trap, and cold vapor atomic fluorescence spectrometry).

## 6 Measured mercury species

The three measured atmospheric mercury species are: (1) gaseous elemental mercury (GEM) or Hg (0); (2) reactive gaseous mercury (RGM), consisting of Hg (II,g) or Hg (I,g)

compounds; and (3) particle-bound Hg (II or I,s) mercury, which we measured only in the fine particle fraction (FPM, PM<sub>2.5</sub>). At present, RGM and FPM, being without standards, are merely operationally defined.

GEM has an average atmospheric lifetime of about one year (Schroeder and Munthe, 1995) which permits near-homogeneous mixing at the hemispheric scale, with a northern hemispheric background of  $\sim 1.5 \text{ ng m}^{-3}$ . GEM is relatively insoluble, and therefore is not wet deposited, and near-surface atmospheric concentrations are unaffected by snow or fog events. GEM comprises  $\sim 97\%$  of the total atmospheric mercury in the troposphere (e.g. Slemr et al., 2003) and has many natural and anthropogenic sources (volcanoes, enriched soils, coal combustion, biomass burning etc.). However, none of these sources are present in central Greenland.

RGM is operationally defined as mercury collected by a KCl coated denuder tube. RGM is typically believed to be dominated by Hg(II) such as HgCl<sub>2</sub>, HgClX and Hg-BrX. RGM is typically rare in the lower troposphere,  $\sim 1\text{--}2 \text{ pg m}^{-3}$  (sub-parts per trillion levels), comprising just  $\sim 1\%$  of total atmospheric mercury. RGM is extremely water soluble, has a high dry deposition rate and so is rapidly removed from the near-surface air (lifetime in the near-surface air is typically just hours). With the exception of active volcanoes, RGM has negligible natural surface sources and is primarily emitted by coal combustion, cement manufacturing, and industrial processes (all absent in central Greenland). RGM can also be produced in-situ by the atmospheric oxidation of gaseous elemental mercury. RGM has the potential to convert to FPM in the presence of sea salts and other aerosols.

FPM is comprised of oxidized mercury bound to fine (PM<sub>2.5</sub>) particles. FPM has a low, but significant, dry deposition rate, and in the absence of precipitation, a significant lifetime in the near-surface air (1–2 days). FPM is the least studied and least measured form of atmospheric mercury. FPM is typically rare ( $\sim 1\text{--}5 \text{ pg m}^{-3}$ ) in the near surface air, but more common near the tropopause. Potential mercury cycling between RGM and FPM has not been fully studied.

## Temperature and sunlight controls of mercury oxidation and deposition

S. Brooks et al.

Title Page

Abstract

Introduction

Conclusions

References

Tables

Figures

⏪

⏩

◀

▶

Back

Close

Full Screen / Esc

Printer-friendly Version

Interactive Discussion



## 7 Results

GEM measurements showed a consistent background level close to northern hemispheric background levels of  $\sim 1.5 \text{ ng m}^{-3}$  (Figs. 1 and 2). GEM depletions below background were generally on the order of  $0.1 \text{ ng m}^{-3}$ , and were most often accompanied by a nearly equal increase in RGM on the order of  $100 \text{ pg m}^{-3}$ . RGM and FPM concentrations ranged from below detection limit (BDL:  $\sim 1.0 \text{ pg m}^{-3}$ ) to  $246.8 \text{ pg m}^{-3}$  and  $151.3 \text{ pg m}^{-3}$ , respectively. Surface snow collected every other day throughout the 2007 and 2008 campaigns averaged  $5.6 \text{ ng l}^{-1}$  for total mercury with no apparent trends. Missing FPM data in 2007 was due to a recurring electrical short in the model 1135 particulate heater unit. Missing GEM periods in 2008 were due to problems associated with the fouling of the in-line soda-lime trap, just upstream of the Tekran 2537a inlet. This problem was eventually traced back to a specific batch of soda-lime. RGM and FPM are reported for this period because, unlike GEM, these measurements are based on a “difference method”. The average diurnal pattern for the measured mercury species for all of the 2007 campaign is shown in Fig. 3.

Br species and chemistry were significantly lower in 2008 than in 2007, even when comparing the same June overlap period. Overall the levels of BrO were lower and less diurnally consistent in 2008 compared to 2007 (Stutz et al., 2011; Liao et al., 2011; Dibb et al., 2010). Total mercury in surface snow was slightly less in 2008 than in 2007 during the overlap period, and GEM showed significantly less variation in 2008.

When comparing concentrations of GEM, RGM, FPM, and BrO, with lifetimes of months, hours, hours to days, and seconds, respectively, it is often difficult to find representative time periods. Periods selected are times of relatively stationary meteorology, or at least multi-day time periods with a similar diurnal meteorological pattern. Both of our selected periods in this section were characterized by light winds, and were bounded by higher wind speeds ( $> 8 \text{ m s}^{-1}$ ) before and after their start/end times.

The first period of interest, 14–19 May 2007, is shown in Fig. 4, with the average diurnal pattern shown in Fig. 5. Here the sun dips to near-zero elevation at night,

### Temperature and sunlight controls of mercury oxidation and deposition

S. Brooks et al.

Title Page

Abstract

Introduction

Conclusions

References

Tables

Figures



Back

Close

Full Screen / Esc

Printer-friendly Version

Interactive Discussion



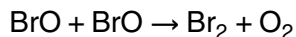
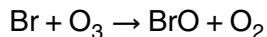
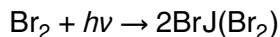
and temperatures were consistently  $< -15^{\circ}\text{C}$ . Winds were generally light ( $1\text{--}6\text{ m s}^{-1}$ ), precipitation was negligible, blowing snow was absent, and skies were generally clear.

For this period we see the obvious signs of typical daily AMDE's. Mercury showed distinct diurnal changes in speciation that appear consistent with midday Br chemistry. GEM often decreased at mid-day, while RGM was increasing. RGM then decreased after midday with deposition to the snow surface. GEM spiked just after peak solar consistent with photoreduction and surface emissions of the recently deposited RGM. Also FPM peaked at night, out of phase with the RGM, due to colder temperatures favoring RGM absorption onto particles. Ozone also showed partial depletions midday, dropping  $\sim 3$  ppb, consistent with Br chemistry, and anti-correlation with RGM.

The second period of interest, 14–19 June 2008, average diurnal pattern is shown in Fig. 6. Winds varied between  $2\text{--}7\text{ m s}^{-1}$ , again precipitation was negligible, blowing snow was absent, and skies were generally clear. The sun was significantly above the horizon 24 hours a day, and temperatures varied from  $-27$  to  $-7^{\circ}\text{C}$ . Here we see a substantially different diurnal pattern (Fig. 6). GEM does not deplete noticeably, but the afternoon photoreduction and surface emissions are still present, as demonstrated by the afternoon GEM enhancements. RGM and FPM are both peaking at “night” during colder ( $< -15^{\circ}\text{C}$ ) temperatures.

## 8 Bromine/Mercury chemistry

If Greenland AMDE chemistry is similar to other polar locations, then under sunlight conditions bromine gas dissociates, catalyzes the destruction of ozone, and oxidizes gaseous elemental mercury (GEM or  $\text{Hg}^0$ ) to reactive gaseous mercury (RGM) via:

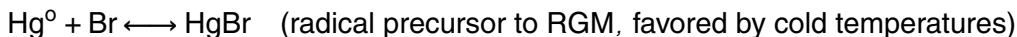


### Temperature and sunlight controls of mercury oxidation and deposition

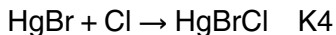
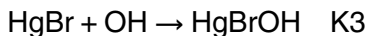
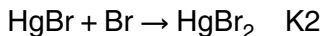
S. Brooks et al.

[Title Page](#)[Abstract](#)[Introduction](#)[Conclusions](#)[References](#)[Tables](#)[Figures](#)[⏪](#)[⏩](#)[◀](#)[▶](#)[Back](#)[Close](#)[Full Screen / Esc](#)[Printer-friendly Version](#)[Interactive Discussion](#)

or



The mercury bromide radical Hg(I) formed in the above mechanism thermally dissociates or may react further with e.g. Br, OH, or Cl, leading to reactive gaseous mercury as Hg(II) (Goodsite et al., 2004). Therefore the fates of HgBr include:



$$\text{Summation } [\text{RGM}] = [\text{HgBr}] (\text{K2 } [\text{Br}] + \text{K3 } [\text{OH}] + \text{K4 } [\text{Cl}]) - \text{K1 } [\text{HgBr}]$$

The newly formed RGM then deposits rapidly to the snow pack with a high deposition velocity ( $\sim 1\text{--}2 \text{ cm s}^{-1}$ ), or becomes bound to airborne particles forming FPM. The global control on this mechanism is thought to be thermal dissociation of HgBr prior to forming the stable RGM (HgBrX). The lifetime against thermal dissociation of HgBr is thought to double with every  $6^{\circ}\text{C}$  drop in temperature (Holmes et al., 2006). Holmes et al. (2006) also concluded that broad uncertainties in the kinetic rates, especially for reactions involving HgBr as a reactant, need to be resolved in order to validate this as a functioning mechanism. Here we will assume this is a valid mechanism, and seek to determine the sunlight and thermal dissociation controls.

In the past it has been difficult to isolate the influences of  $J(\text{Br}_2)$ , and the thermal decomposition lifetime of HgBr. At coastal locations  $\text{Br}_2$  concentrations vary with marine verses continental air, and rapidly changing sea ice conditions. Non-homogeneous upwind conditions may transport RGM and/or Br into the measurement location. Periods

## Temperature and sunlight controls of mercury oxidation and deposition

S. Brooks et al.

Title Page

Abstract

Introduction

Conclusions

References

Tables

Figures

⏪

⏩

◀

▶

Back

Close

Full Screen / Esc

Printer-friendly Version

Interactive Discussion



of varying winds, which affect boundary layer depths and mixing, confound efforts to isolate these variables. For two distinct sub-periods at Summit, Greenland the above confounding effects are all absent or minimal.

The two sub-periods (14–19 May 2007 and 7–13 June 2008) mentioned previously, best demonstrate the controls of solar ( $J(\text{Br}_2)$ ) and air temperature. During both periods winds were generally light ( $<1\text{--}6\text{ m s}^{-1}$  during 7–13 May and  $2\text{--}7\text{ m s}^{-1}$  during 7–13 June), precipitation was negligible, blowing snow was absent, and skies were generally clear. Both of these periods are bounded by higher wind speeds ( $>8\text{ m s}^{-1}$ ) at their beginnings and endings. Figures 7 and 8 show the RGM from our selected periods, air temperature and  $J(\text{Br}_2)$  for the photodissociation production of monatomic Br.

During the period 7–13 May (Fig. 7), the air temperature was consistently below  $-15^\circ\text{C}$  and RGM was strongly correlated to  $J(\text{Br}_2)$  and decoupled from temperature. RGM peaks were well defined at maximum solar elevations with broad FPM enhancements at near-zero solar elevations (Fig. 3). Gaseous elemental mercury (GEM) concentrations (Fig. 3) were approximately Northern Hemisphere background levels,  $\sim 1.5\text{ ng m}^{-3}$ , with small decreases in concentrations during midday RGM production, and enhancements from photoreduction coincident with newly deposited RGM.

During the period 7–13 June (Fig. 8), the air temperature varied from  $-27$  to  $-7^\circ\text{C}$ , and thermal dissociation of  $\text{HgBr}$  dominated over the formation of  $\text{HgBrX}$  during the higher midday air temperatures.  $J(\text{Br}_2)$  was well above zero over the 24 hours/day of sunlight. Therefore, RGM enhancements were decoupled from solar  $J(\text{Br}_2)$  and were strongly anti-correlated to air temperatures. GEM concentrations (Fig. 6) showed little decrease at the on-set of RGM enhancements, and GEM enhancements were bimodal with enhancements from photoreduction coincident with newly deposited RGM, and again from photoreduction broadly centered around daily maximum solar.

Based on these observations we conclude that by assuming consistent concentrations of X (Br, Cl, OH) in the reactions  $\text{HgBr} + \text{X} \rightarrow \text{HgBrX}$ , we can define the solar elevations and temperatures where GEM conversion to RGM should occur. We calculate

## Temperature and sunlight controls of mercury oxidation and deposition

S. Brooks et al.

Title Page

Abstract

Introduction

Conclusions

References

Tables

Figures

⏪

⏩

◀

▶

Back

Close

Full Screen / Esc

Printer-friendly Version

Interactive Discussion

that GEM oxidation to RGM (Hg(II)) atop the Greenland ice cap requires solar elevation angles  $> 5$  degrees and air temperatures  $< -15^{\circ}\text{C}$ . We expect this assumption to fail at coastal locations where Br and Cl are episodically enriched. At Point Barrow, Alaska, at a similar latitude as Summit, Greenland, we have measured significant concentrations of RGM ( $> 10\text{ pg m}^{-3}$ ) up to a temperature of  $-6^{\circ}\text{C}$  (Lindberg et al., 2002).

Br is the only oxidant known to be capable of oxidizing GEM to RGM rapidly enough to create the pronounced diurnal variations of RGM we observed. Nighttime minima of RGM suggest that deposition to the snow is a strong sink, and imply an RGM lifetime at Summit during our campaign in the 3–10 h range. Assuming that a 7 h lifetime is short enough that RGM production is roughly balanced by deposition allows estimation of Br from the steady state relationship:

$$[\text{Br}] = \frac{[\text{RGM}]}{[\text{GEM}] \cdot k_{\text{Br}+\text{GEM}} \cdot (7\text{ h})}$$

It should be noted that  $k_{\text{Br}+\text{GEM}}$  is not well established, with determinations reported by Ariya et al. (2002) and Donohoue et al. (2006) as  $(3.2 \pm 0.3) \times 10^{12}$  and  $(3.6 \pm 50\%) \times 10^{-13}\text{ cm}^3\text{ molecule}^{-1}\text{ s}^{-1}$ , respectively. As these rates differ by an order of magnitude, the estimated [Br] is highly uncertain. Using  $[\text{RGM}] = 100\text{ pg m}^{-3}$ ,  $[\text{GEM}] = 1500\text{ pg m}^{-3}$ , [Br] equates to  $5.8 \times 10^5$  and  $5.2 \times 10^6\text{ molecule cm}^{-3}$  ( $\sim 0.03$  and  $0.3\text{ pptv}$ ) based on the rates of Ariya et al. (2002) and Donohoue et al. (2006), respectively.

High correlations between RGM and BrO, for any extended period of time, were rare at Summit. Likely reasons for the lack of correlation include: RGM deposits rapidly to the snow surface except under very light winds, and RGM is not formed above  $-15^{\circ}\text{C}$ , or when the solar elevation is less than 5 degrees. There was only one multi-day period during the entire study when wind speeds were consistently below  $3\text{ m s}^{-1}$ . The temperatures were also cold, varying from a period high of  $-12^{\circ}\text{C}$  to a low of  $-24^{\circ}\text{C}$ , sufficiently for RGM production under 24 h sunlight ( $> 5$  degrees). This period, 8, 9, and 10 June is shown in Fig. 9. Note that RGM does not disappear at night due to 24 h sunlight.

## Temperature and sunlight controls of mercury oxidation and deposition

S. Brooks et al.

[Title Page](#)[Abstract](#)[Introduction](#)[Conclusions](#)[References](#)[Tables](#)[Figures](#)[⏪](#)[⏩](#)[◀](#)[▶](#)[Back](#)[Close](#)[Full Screen / Esc](#)[Printer-friendly Version](#)[Interactive Discussion](#)

A single snow core was obtained using a pre-clean Kovacs coring instrument at Summit in June 2008. Total Hg in the firn was measured every  $\sim 30$  cm to a depth of 7.1 m. Total Hg at depth (below the first meter) averaged  $3.0 \text{ g l}^{-1}$ , with no recognizable pattern or trend with increasing depth.

## 9 Discussion and extrapolation to the vast Greenland ice sheet

The Greenland ice sheet covers an area of  $\sim 14$  million  $\text{km}^2$  with an annual snow accumulation rate of  $\sim 300 \text{ kg m}^{-2}$  (Bales et al., 2001). From our snow coring measurements, total mercury averages  $3.0 \text{ ng l}^{-1}$  at depth. From these values we calculate that the Greenland ice sheet sequesters  $\sim 13$  metric tons Hg per year at depth. We postulate that, while the vast majority of deposited RGM is photoreduced and re-emitted within hours, a small fraction of deposited mercury is buried by falling or drifting snow below the sunlit zone (top  $\sim 10$  cm) becoming sequestered long-term.

We assume here that the chemical composition of the near-surface air over the vast Greenland ice sheet does not vary significantly from those measured at Summit, giving a temperature cutoff for RGM formation at  $\sim -15^\circ\text{C}$ . We expect this assumption to fail at coastal locations near the sea ice where Br is significantly more enriched.

The production of RGM over snow surfaces appears to depend on solar elevation angle  $>5$  degrees and air temperatures  $< -15^\circ\text{C}$ . While  $J(\text{Br}_2)$  is not thought to vary significantly at a given ice cap location from year to year, air temperature may vary significantly and affect overall RGM production and subsequent deposition.

Using solar elevation  $> 5$  degrees and air temperatures  $< -15^\circ\text{C}$  as the criteria for RGM production, we generated the RGM formation maps shown in Fig. 10. RGM production is predicted in the southern half of the ice cap from the beginning of January, and proceeds northward during February and covering all of Greenland by March and April. In May, average temperatures rise well above  $-15^\circ\text{C}$  in southern Greenland and at the lower coastal elevations. By June, RGM production is restricted to the higher ice cap elevations. These conditions persist through the summer months. In October, the

## Temperature and sunlight controls of mercury oxidation and deposition

S. Brooks et al.

Title Page

Abstract

Introduction

Conclusions

References

Tables

Figures

⏪

⏩

◀

▶

Back

Close

Full Screen / Esc

Printer-friendly Version

Interactive Discussion



area of RGM production begins to increase with dropping temperatures. By November, RGM production halts in the Northern half of Greenland due to lack of sunlight. In December, only the southern half of Greenland experiences RGM production.

Regional warming at high latitudes will likely reduce RGM production and deposition.

Should the Greenland ice cap warm considerably, the periods of solar elevation > 5 degrees with temperatures below  $< -15^{\circ}\text{C}$  would decrease in duration. This would likely lead to lower rates of RGM formation and lower deposition rates. On the other hand, warmer temperatures could result in increased snow accumulation and increased Hg burial rates.

## 10 Conclusions

Halogen (such as bromine, Br) chemistry is normally associated with marine boundary layers, not remote high-altitude ice sheets. However, at Summit, Greenland, we have conclusively detected bromine and mercury chemistry in the near surface air. We conclude that the fate of the mercury-bromine radical (HgBr) is further oxidation to stable RGM (HgBr<sub>2</sub>, HgBrOH, HgBrCl, etc.), or thermal decomposition. These fates appear to be controlled by the availability of Br, OH, Cl, etc. to produce RGM, versus the lifetime of HgBr by thermal dissociation. At Summit, the availability of Br appears to be controlled by J(Br<sub>2</sub>), requiring a sun angle of > 5 degrees, while the formation of RGM from HgBr requires a temperature  $< -15^{\circ}\text{C}$ .

At Summit most of the deposited RGM is readily photoreduced and re-emitted to the air as GEM. However, a very small fraction becomes buried at depth resulting in an estimated annual sequestration of ~ 13 metric tons Hg per year for the Greenland ice sheet.

*Acknowledgements.* We would like to acknowledge the Summit staff for their support. Maria Hörhold and Kristina Sorg for their assistance obtaining the firn core with the Kovacs hand corer. We thank NSF for their support and NOAA/ESRL/GMD for their archived meteorology data.

## Temperature and sunlight controls of mercury oxidation and deposition

S. Brooks et al.

Title Page

Abstract

Introduction

Conclusions

References

Tables

Figures

⏪

⏩

◀

▶

Back

Close

Full Screen / Esc

Printer-friendly Version

Interactive Discussion



## References

- Ariya, P. A., Khalizov, A., and Gidas, A.: Reactions of Gaseous Mercury with Atomic and Molecular Halogens: Kinetics, Product Studies, and Atmospheric Implications, *J. Phys. Chem. A*, 106, 7310–7320, 2002.
- 5 Ariya, P. A., Dastoor, A., Amyot, M., Schroeder, W., Barrie, L., Anlauf, K., Raofie, F., Ryzhkov, A., Davignon, D., Lalonde, J., and Steffen, A.: Arctic: A sink for mercury, *Tellus*, 56B, 397–403, 2004.
- Bales, R. C., McConnell, J. R., Mosley-Thompson, E., and Csatho, B.: Accumulation over the Greenland ice sheet from historical and recent records. *J. Geophys. Res.-Atmos*, 106(D24), 33813–33826, 2001.
- 10 Banic, C., Beauchamp, S. T., Tordon, R. J., Schroeder, W. H., Steffen, A., and Anlauf, K. A.: Vertical distribution of gaseous elemental mercury in Canada, *J. Geophys. Res.*, 108(D9), 4264, doi:10.1029/2002JD002116, 2003.
- Bartels-Rausch, T., Jöri, M., and Ammann, M.: Adsorption of mercury on crystalline ice, Annual Report, Laboratory for radiochemistry and environmental chemistry, Paul Scherrer Institut, Villigen, Switzerland, 2002.
- 15 Berg T., Sekkesæter, S., Steinnes, E., Valdal, A., and Wibetoe, G.: Arctic springtime depletion of mercury in the European Arctic as observed at Svalbard, *Sci. Total Environ.*, 304, 43–51, 2003.
- 20 Boutron, C. F., Vandal, G. M., Fitzgerald, W. F., and Ferrari, C. P.: A forty-year record of mercury in central Greenland snow, *Geophys. Res. Lett.*, 25, 3315–3318, 1998.
- Brooks, S., Saiz-Lopez, A., Skov, H., Lindberg, S., Plane, J. M. C., and Goodsite, M. E.: The mass balance of mercury in the springtime polar environment, *Geophys. Res. Lett.*, 33, L13812, doi:10.1029/2005GL025525, 2006.
- 25 Brooks, S., Arimoto, R., Lindberg, S., and Southworth, G.: Antarctic polar plateau snow surface conversion of deposited oxidized mercury to gaseous elemental mercury with fractional long-term burial, *Atmos. Environ.*, 42, 2877–2884, 2008.
- Dibb, J. E., Ziemba, L. D., Luxford, J., and Beckman, P.: Bromide and other ions in the snow, firn air, and atmospheric boundary layer at Summit during GSHOX, *Atmos. Chem. Phys.*, 10, 9931–9942, doi:10.5194/acp-10-9931-2010, 2010.
- 30 Dommergue, A., Ferrari, C. P., Gauchard, P.-A., Boutron, C. F., Poissant, L., Pilote, M., Jitaru, P., and Adams, F.: The fate of mercury species in a sub-arctic snow-pack during snowmelt,

### Temperature and sunlight controls of mercury oxidation and deposition

S. Brooks et al.

Title Page

Abstract

Introduction

Conclusions

References

Tables

Figures

⏪

⏩

◀

▶

Back

Close

Full Screen / Esc

Printer-friendly Version

Interactive Discussion



**Temperature and  
sunlight controls of  
mercury oxidation  
and deposition**

S. Brooks et al.

[Title Page](#)[Abstract](#)[Introduction](#)[Conclusions](#)[References](#)[Tables](#)[Figures](#)[⏪](#)[⏩](#)[◀](#)[▶](#)[Back](#)[Close](#)[Full Screen / Esc](#)[Printer-friendly Version](#)[Interactive Discussion](#)

- Geophys. Res. Lett., 30, 1621, doi:10.1029/2003GL017308, 2003.
- Dommergue, A., Sprovieri, F., Pirrone, N., Ebinghaus, R., Brooks, S., Courteaud, J., and Ferrari, C. P.: Overview of mercury measurements in the Antarctic troposphere, *Atmos. Chem. Phys.*, 10, 3309–3319, doi:10.5194/acp-10-3309-2010, 2010.
- 5 Donohoue, D. L., Bauer, D., Cossairt, B., and Hynes, A. J.: Temperature and pressure dependent rate coefficients for the reaction of Hg with Br and the reaction of Br with Br: A pulsed laser photolysis-pulsed laser induced fluorescence study, *J. Phys. Chem. A*, 110, 21, 6623–6632, 2006.
- Ebinghaus, R., Kock, H. H., Temme, C., Einax, J. W., Lowe, A. G., Richter, A., Burrows, J. P.,  
10 and Schroeder, W. H.: Antarctic springtime depletion of atmospheric mercury, *Environ. Sci. Technol.*, 36, 1238–1244, 2002.
- Fäin, X., Ferrari, C. P., Dommergue, A., Albert, M., Battle, M., Arnaud, L., Barnola, J.-M., Cairns, W., Barbante, C., and Boutron, C.: Mercury in the snow and firn at Summit Station, Central Greenland, and implications for the study of past atmospheric mercury levels, *Atmos. Chem. Phys.*, 8, 3441–3457, doi:10.5194/acp-8-3441-2008, 2008.
- 15 Ferrari, C. P., Dommergue, A., and Boutron, C. F.: Profiles of mercury in the snow pack at Station Nord, Greenland shortly after polar sunrise. *Geophys. Res. Lett.*, 31, L03401, doi:10.1029/2003GL018961, 2004.
- Fitzgerald, W. F. and Gill, G. A.: Sub-nanogram determination of mercury by a 2-stage gold amalgamation and gas-phase detection applied to atmospheric analysis, *Anal. Chem.*, 51, 1714–1720, 1979.
- 20 Goodsite, M. E., Plane J. M. C., and Skov, H.: A theoretical study of the oxidation of Hg-0 to HgBr<sub>2</sub> in the troposphere, *Environ. Sci. Technol.*, 38(6), 1772–1776, 2004.
- Holmes, C. D., Jacob, D. J., and Yang, X.: Global lifetime of elemental mercury against oxidation by atomic bromine in the free troposphere, *Geophys. Res. Lett.*, 33, 20, L20808, doi:10.1029/2006GL027176, 2006.
- 25 King, M. D. and Simpson, W. R.: Extinction of UV radiation in Arctic snow at Alert, Canada (82° N), *J. Geophys. Res.*, 106, 12499–12507, 2001.
- Lalonde, J. D., Poulain, A. J., and Amyot, M.: The role of mercury redox reactions in snow on snow-to-air mercury transfer, *Environ. Sci. Technol.*, 36, 174–178, 2002.
- 30 Lalonde, J. D., Amyot, M., Doyon, M. R., and Auclair, J. C.: Photo-induced Hg(II) reduction in snow from the remote and temperate Experimental Lakes Area (Ontario, Canada), *J. Geophys. Res-Atmos.*, 108(D6), 4200, doi:10.1029/2001JD001534, 2003.

**Temperature and  
sunlight controls of  
mercury oxidation  
and deposition**

S. Brooks et al.

Title Page

Abstract

Introduction

Conclusions

References

Tables

Figures



Back

Close

Full Screen / Esc

Printer-friendly Version

Interactive Discussion



Landis, M., Stevens, R. K., Schaedlich, F., and Prestbo, E. M.: Development and characterization of an annular denuder methodology for the measurement of divalent inorganic reactive gaseous mercury in ambient air, *Environ. Sci. Technol.*, 36, 3000–3009, 2002.

Lindberg, S. E., Brooks, S. B., Lin, C. J., Scott, K. J., Landis, M. S., Stevens, R. K., Goodsite, M., and Richter, A.: Dynamic Oxidation of Gaseous Mercury in the Arctic Troposphere at Polar Sunrise, *Environ. Sci. Technol.*, 36, 1245–1256, 2002.

Liao, J., Huey, L. G., Tanner, D. J., Brooks, S., Dibb, J. E., Stutz, J., Thomas, J., Lefer, B., Haman, C., and Gorham, K.: Observations of hydroxyl and peroxy radicals and the impact of BrO at Summit, Greenland in 2007 and 2008, *Atmos. Chem. Phys. Discuss.*, in preparation, 2011.

Lu, J. Y., Schroeder, W. H., Berg, T., Munthe, J., Schneeberger, D., and Schaedlich, F.: A device for sampling and determination of total particulate mercury in ambient air, *Anal. Chem.*, 70, 2403–2408, 1998.

Mann, J. L., Long, S. E., Shuman, C. A., and Kelly, W. R.: Determination of Mercury content in a shallow firn core from Greenland by isotope dilution inductively coupled plasma mass spectrometry, *Water Air Soil Poll.*, 163, 19–32, 2005.

Schroeder, W. H. and Munthe, J.: Atmospheric mercury – an overview, *Atmos. Environ.*, 32, 5, 809–822, 1995.

Schroeder, W. H., Anlauf, K. G., Barrie, L. A., Lu, J. Y., Steffen, A., Schneeberger, D. R., and Berg, T.: Arctic springtime depletion of mercury, *Nature*, 394, 331–332, 1998.

Skov, H., Christensen, J. H., Goodsite, M. E., Heidam, N. Z., Jensen, B., Wahlin, P., and Geernaert, G.: Fate of elemental mercury in the Arctic during atmospheric mercury depletion episodes and the load of atmospheric mercury to the arctic, *Environ. Sci. Technol.*, 38, 2373–2382, 2004.

Sjostedt, S. J., Huey, L. G., Tanner, D. J., Pieschl, J., Chen, G., Dibb, J. E., Lefer, B., Hutterli, M. A., Beyersdorf, A. J., Blake, N. J., Blake, D. R., Sueper, D., Ryerson, T., Burkhardt, J., and Stohl, A.: Observations of hydroxyl and the sum of peroxy radicals at Summit, Greenland during summer 2003, *Atmos. Environ.*, 41(24), 5122–5137, doi:10.1016/j.atmosenv.2006.06.065, 2007.

Slemr, F., Brunke, E. G., Ebinghaus, R., Temme, C., Munthe, J., Wangberg, I., Schroeder, W., Steffen, A., and Berg, T.: Worldwide trend of atmospheric mercury since 1977, *Geophys. Res. Lett.*, 30(10), 1516, doi:10.1029/2003GL016954, 2003.

Steffen A., Schroeder, W. H., Macdonald, R., Poissant, L., and Konoplev, A.: Mercury in the arc-

tic atmosphere: an analysis of eight years of measurements of GEM at Alert (Canada) and a comparison with observations at Amderma (Russia) and Kuujuarapik (Canada), STOTEN, 342, 185–198, 2005.

5 Steffen, A., Douglas, T., Amyot, M., Ariya, P., Aspmo, K., Berg, T., Bottenheim, J., Brooks, S., Cobbett, F., Dastoor, A., Dommergue, A., Ebinghaus, R., Ferrari, C., Gardfeldt, K., Goodsite, M. E., Lean, D., Poulain, A. J., Scherz, C., Skov, H., Sommar, J., and Temme, C.: A synthesis of atmospheric mercury depletion event chemistry in the atmosphere and snow, Atmos. Chem. Phys., 8, 1445–1482, doi:10.5194/acp-8-1445-2008, 2008.

10 Stutz, J., Thomas, J. L., Hurlock, S. C., Schneider, M., von Glasow, R., Piot, M., Gorham, K., Burkhardt, J. F., Ziemba, L., and Dibb, J.: Observations of BrO at Summit, Greenland, Atmos. Chem. Phys. Discuss., in preparation, 2011.

Tackett, P. J., Cavender, A. E., Keil, A. D., Shepson, P. B., Bottenheim, J. W., Morin, S., Deary, J., Steffen, A., and Doerge, C.: A study of the vertical scale of halogen chemistry in the Arctic troposphere during Polar Sunrise at Barrow, Alaska, J. Geophys. Res., 112, D07306, doi:10.1029/2006JD007785, 2007.

15 Vandal, G. M., Fitzgerald, W. F., Boutron, C. F., and Candelone, J.P.: Variations in mercury deposition to Antarctica over the past 34000 years, Nature, 362, 621–623, 1993.

**Temperature and  
sunlight controls of  
mercury oxidation  
and deposition**

S. Brooks et al.

Title Page

Abstract

Introduction

Conclusions

References

Tables

Figures

⏪

⏩

◀

▶

Back

Close

Full Screen / Esc

Printer-friendly Version

Interactive Discussion



## Temperature and sunlight controls of mercury oxidation and deposition

S. Brooks et al.

**Table 1.** All mercury speciation measurements at Summit, Greenland. Dates are 13 May–15 June 2007, and 6 June–17 July 2008. Below Detection limit (B.D.L.) denotes that values were below the detection limit ( $< 1.0 \text{ pg m}^{-3}$ ) of the instrument. Also shown is total mercury in surface snow collected every other day.

		Average	Standard Deviation	Minimum	Maximum	Coeff. Of Variation
2007	GEM ( $\text{ng m}^{-3}$ )	1.31	0.21	1.04	3.49	0.16
	RGM ( $\text{pg m}^{-3}$ )	41.6	42.9	B.D.L.	246.8	1.03
	FPM ( $\text{pg m}^{-3}$ )	37.2	31.9	B.D.L.	151.3	0.86
2008	GEM ( $\text{ng m}^{-3}$ )	1.45	0.11	1.12	1.88	0.08
	RGM ( $\text{pg m}^{-3}$ )	13.2	19.0	B.D.L.	122.6	1.44
	FPM ( $\text{pg m}^{-3}$ )	6.7	8.7	B.D.L.	61.5	1.30
All Surface Snow		$5.6 \text{ ng l}^{-1}$	$4.3 \text{ ng l}^{-1}$	$1.3 \text{ ng l}^{-1}$	$22.9 \text{ ng l}^{-1}$	0.77

Title Page

Abstract

Introduction

Conclusions

References

Tables

Figures

⏪

⏩

◀

▶

Back

Close

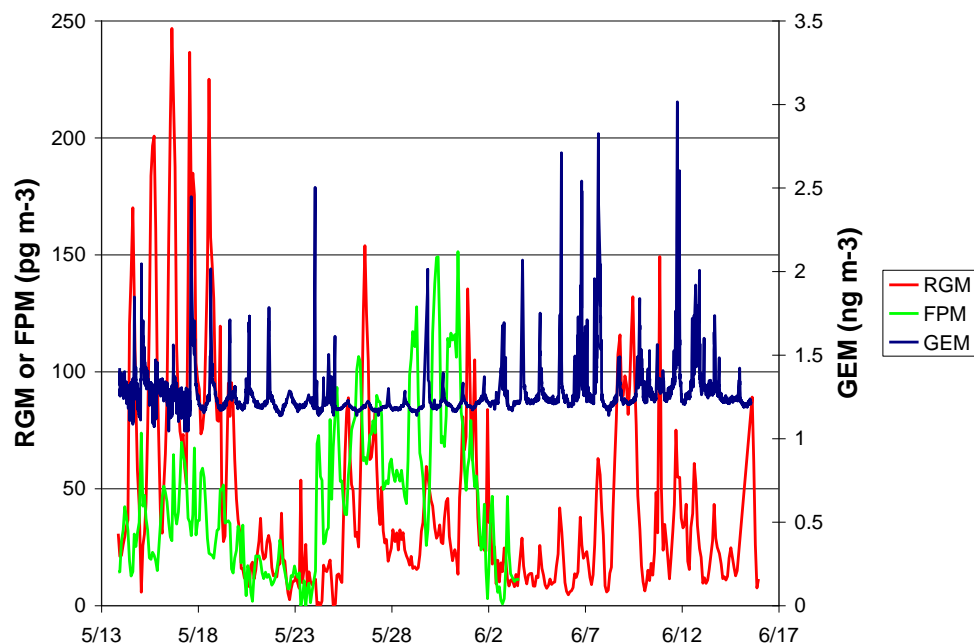
Full Screen / Esc

Printer-friendly Version

Interactive Discussion

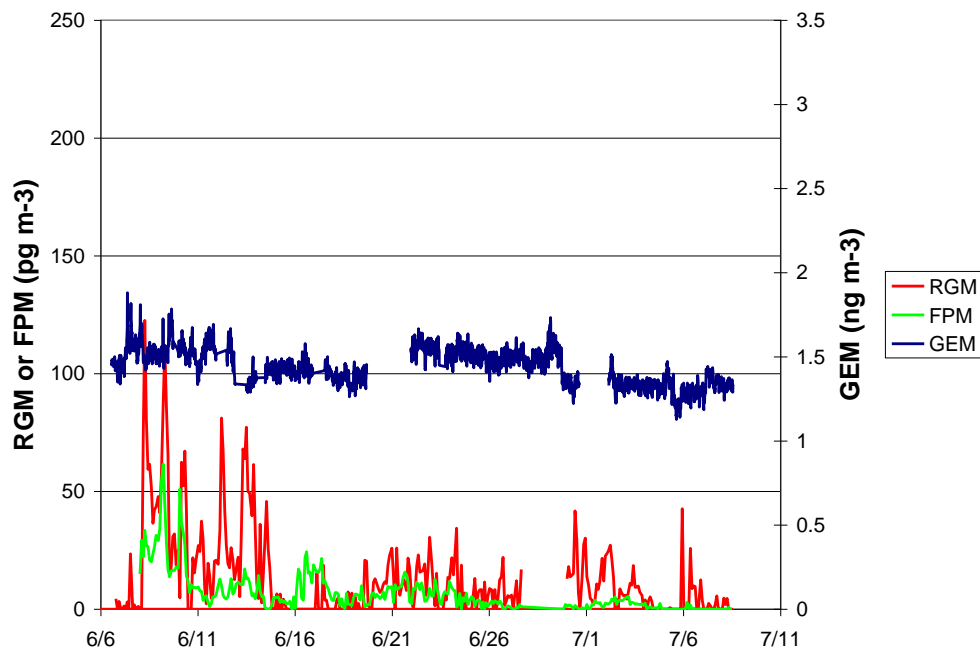
**Temperature and  
sunlight controls of  
mercury oxidation  
and deposition**

S. Brooks et al.

**Fig. 1.** All mercury speciation data from the 2007 campaign.[Title Page](#)[Abstract](#)[Introduction](#)[Conclusions](#)[References](#)[Tables](#)[Figures](#)[⏪](#)[⏩](#)[◀](#)[▶](#)[Back](#)[Close](#)[Full Screen / Esc](#)[Printer-friendly Version](#)[Interactive Discussion](#)

**Temperature and  
sunlight controls of  
mercury oxidation  
and deposition**

S. Brooks et al.

**Fig. 2.** All mercury speciation data from the 2008 campaign.[Title Page](#)[Abstract](#)[Introduction](#)[Conclusions](#)[References](#)[Tables](#)[Figures](#)[◀](#)[▶](#)[◀](#)[▶](#)[Back](#)[Close](#)[Full Screen / Esc](#)[Printer-friendly Version](#)[Interactive Discussion](#)

**Temperature and  
sunlight controls of  
mercury oxidation  
and deposition**

S. Brooks et al.

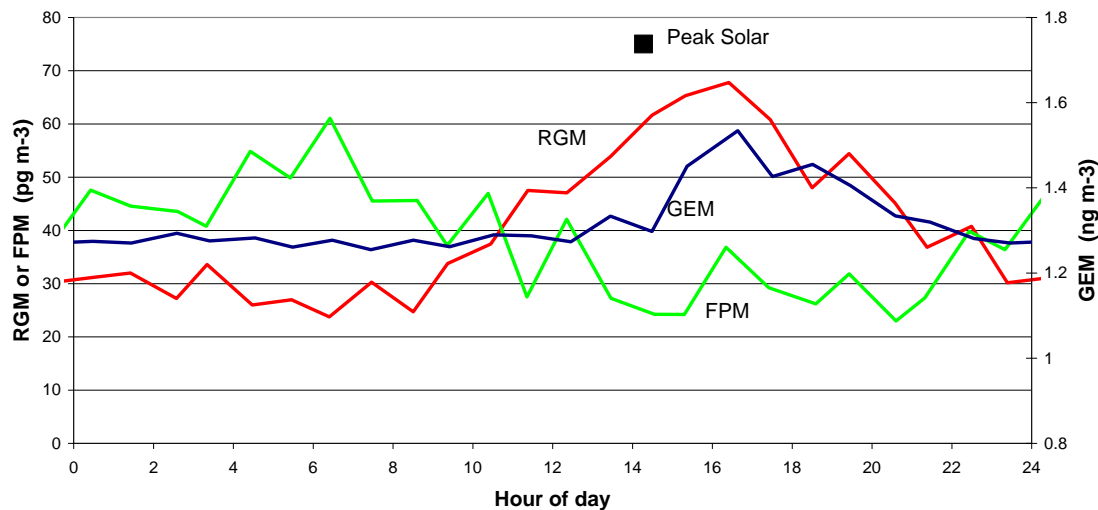


**Fig. 3.** Hourly diurnal averages for all 2007 campaign measurements.

[Title Page](#)[Abstract](#)[Introduction](#)[Conclusions](#)[References](#)[Tables](#)[Figures](#)[⏪](#)[⏩](#)[◀](#)[▶](#)[Back](#)[Close](#)[Full Screen / Esc](#)[Printer-friendly Version](#)[Interactive Discussion](#)

**Temperature and  
sunlight controls of  
mercury oxidation  
and deposition**

S. Brooks et al.

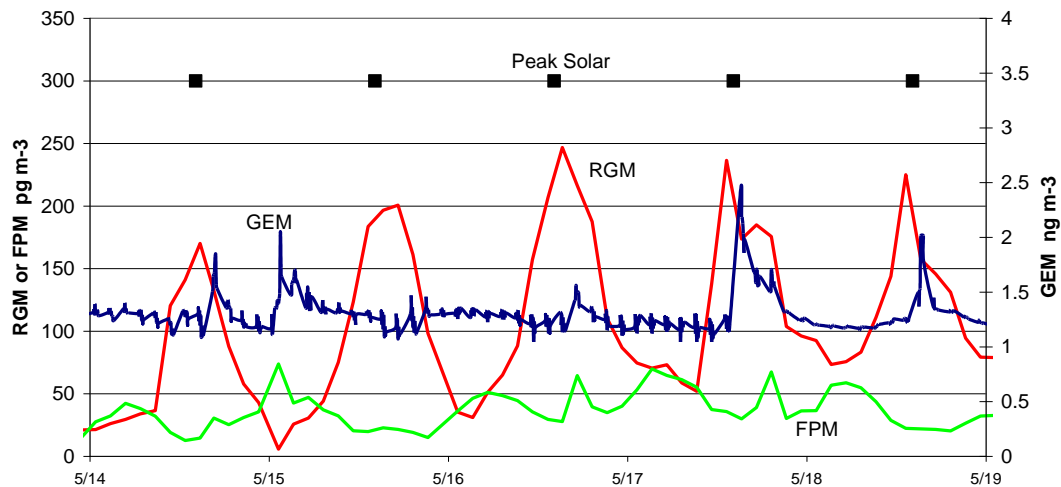


**Fig. 4.** Reactive gaseous mercury (RGM), fine particulate mercury (FPM), gaseous elemental mercury (GEM), and times of peak solar elevation at Summit, Greenland, 14–19 May 2007.

## Temperature and sunlight controls of mercury oxidation and deposition

S. Brooks et al.

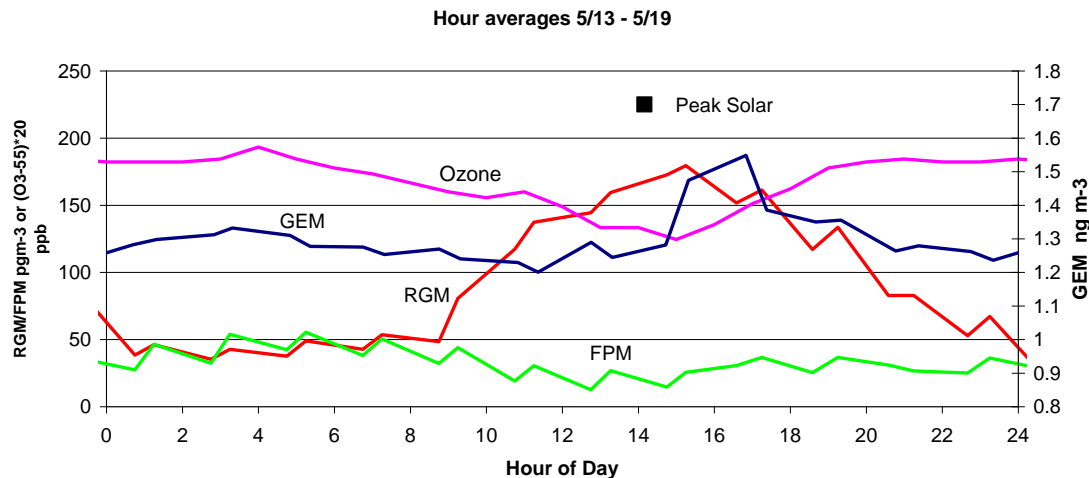


**Fig. 5.** Diurnal hourly averages of RGM, GEM, FPM and Ozone at Summit, 14–19 May 2007. Daily RGM peaks with maximum solar elevation.

Title Page

Abstract

Introduction

Conclusions

References

Tables

Figures

◀

▶

◀

▶

Back

Close

Full Screen / Esc

Printer-friendly Version

Interactive Discussion

**Temperature and  
sunlight controls of  
mercury oxidation  
and deposition**

S. Brooks et al.

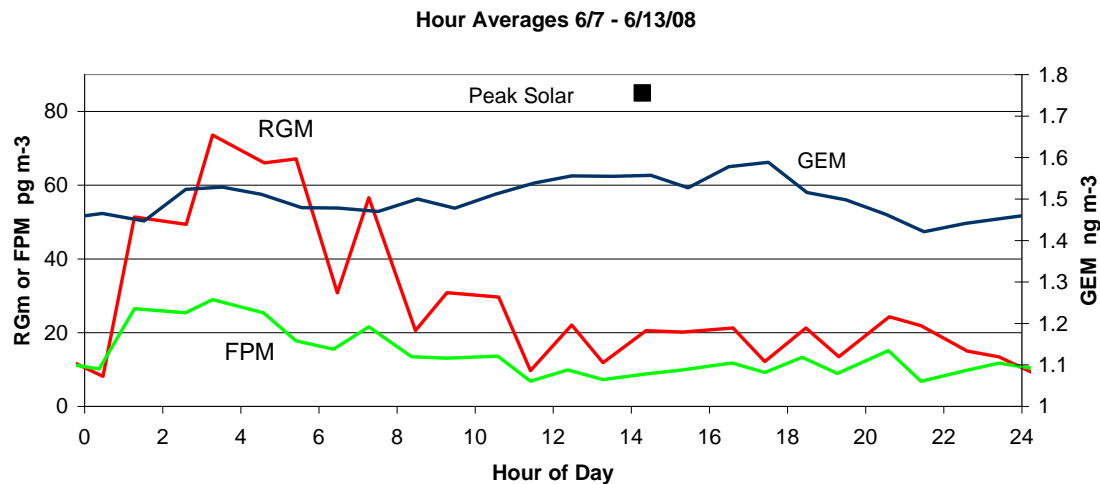


**Fig. 6.** Diurnal hourly averages of RGM, GEM and FPM at Summit, 7–13 June 2008. Daily RGM peaks with colder “nighttime” temperatures.

[Title Page](#)[Abstract](#)[Introduction](#)[Conclusions](#)[References](#)[Tables](#)[Figures](#)[⏪](#)[⏩](#)[◀](#)[▶](#)[Back](#)[Close](#)[Full Screen / Esc](#)[Printer-friendly Version](#)[Interactive Discussion](#)

**Temperature and  
sunlight controls of  
mercury oxidation  
and deposition**

S. Brooks et al.

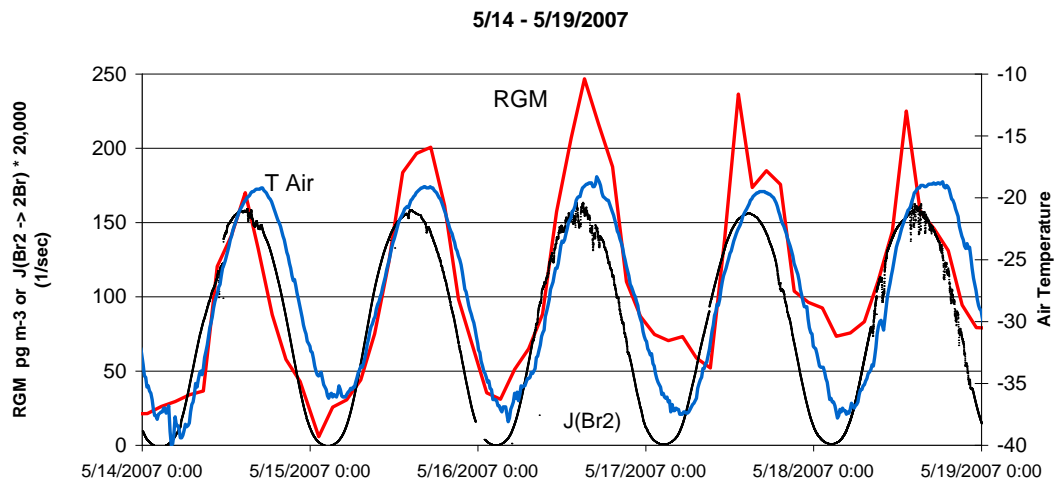


**Fig. 7.** Reactive gaseous mercury (RGM),  $J(\text{Br}_2 + h\nu \rightarrow 2\text{Br})$ , and air temperature at Summit, Greenland, 14–19 May 2007. Under uniformly cold  $< -15^\circ\text{C}$  conditions RGM enhancements are well correlated to Br production ( $J(\text{Br}_2)$ ).  $J(\text{Br}_2)$  is very close to zero at near-zero solar angles.

Title Page

Abstract

Introduction

Conclusions

References

Tables

Figures

◀

▶

◀

▶

Back

Close

Full Screen / Esc

Printer-friendly Version

Interactive Discussion

Temperature and  
sunlight controls of  
mercury oxidation  
and deposition

S. Brooks et al.

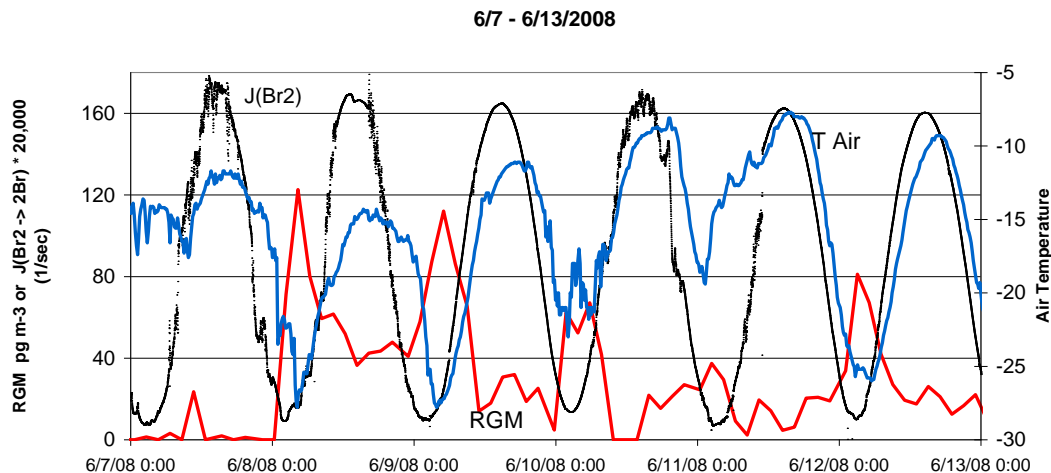


**Fig. 8.** Reactive gaseous mercury (RGM),  $J(\text{Br}_2 + h\nu \rightarrow 2\text{Br})$ , and air temperature at Summit, Greenland, 7–13 June 2008. Under significant 24 h sunlight  $J(\text{Br}_2)$  terms are consistent above zero. RGM concentrations are anti-correlated to air temperature, indicating the importance of cold temperatures on the lifetime of HgBr, allowing the formation of HgBrX (RGM).

Title Page

Abstract

Introduction

Conclusions

References

Tables

Figures

◀

▶

◀

▶

Back

Close

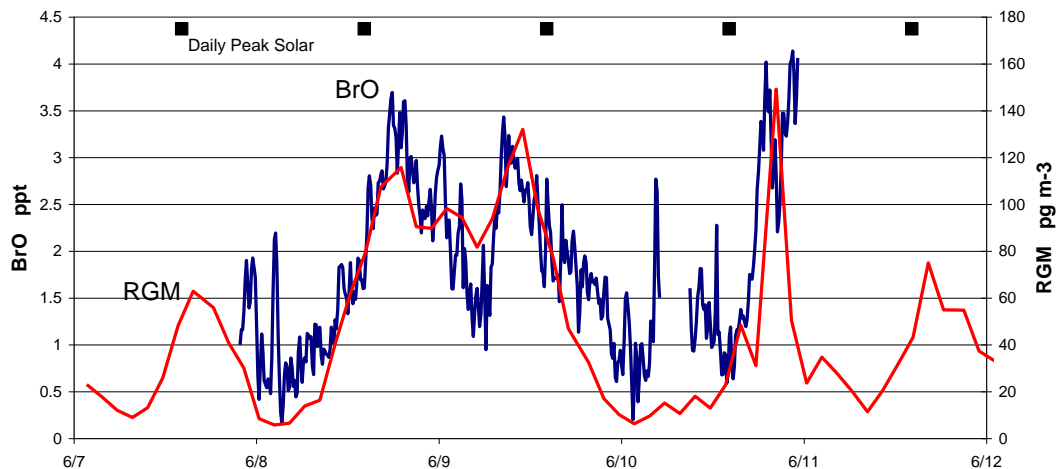
Full Screen / Esc

Printer-friendly Version

Interactive Discussion

**Temperature and  
sunlight controls of  
mercury oxidation  
and deposition**

S. Brooks et al.

**Fig. 9.** RGM and BrO from 2007.[Title Page](#)[Abstract](#)[Introduction](#)[Conclusions](#)[References](#)[Tables](#)[Figures](#)[⏪](#)[⏩](#)[◀](#)[▶](#)[Back](#)[Close](#)[Full Screen / Esc](#)[Printer-friendly Version](#)[Interactive Discussion](#)

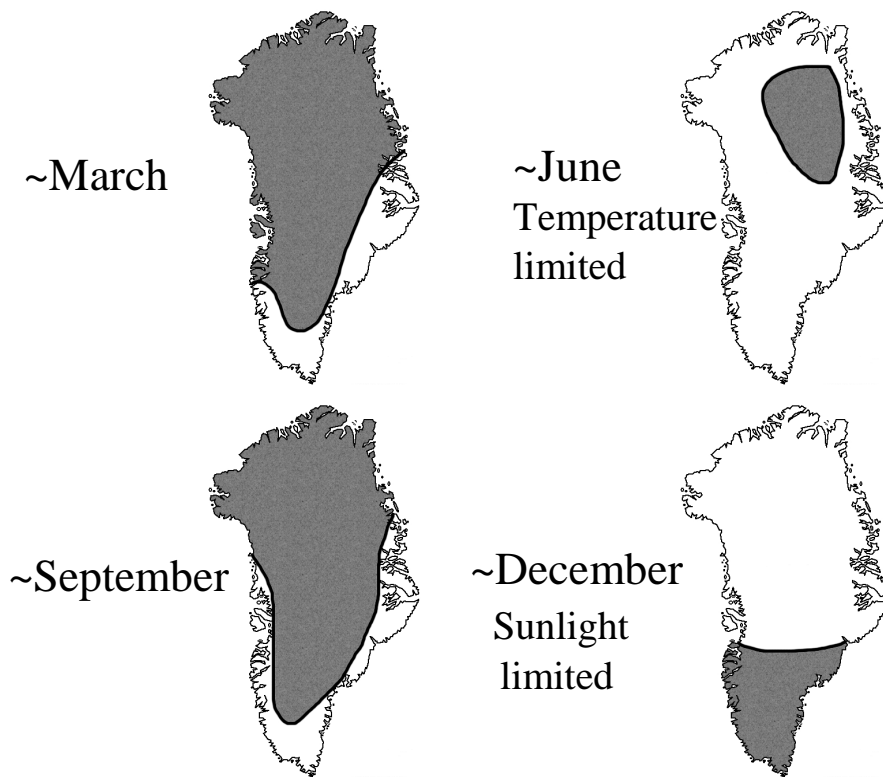


**Fig. 10.** Seasonal plots of the area of the Greenland ice cap where solar elevation exceeds 7 degrees and where the average daily low temperature is  $< -15^{\circ}\text{C}$  (shaded).

**Temperature and  
sunlight controls of  
mercury oxidation  
and deposition**

S. Brooks et al.

Title Page

Abstract

Introduction

Conclusions

References

Tables

Figures

◀

▶

◀

▶

Back

Close

Full Screen / Esc

Printer-friendly Version

Interactive Discussion

